

2 Measurement Uncertainties in Wear Rates

3 David L. Burris · W. Gregory Sawyer

4 Received: 6 May 2009 / Accepted: 22 June 2009
5 © Springer Science+Business Media, LLC 2009

6 **Abstract** Measurement uncertainties are vital to discus-
7 sions of differences in measured values, yet they scarcely
8 accompany discussions of wear and wear rates in the tri-
9 bology literature. In this methods article, approaches to
10 calculate uncertainties in single-point and steady-state wear
11 rates are presented. The analysis includes analytical treat-
12 ments of uncertainties for typical macroscopic tribology
13 instrumentation. A fully statistical treatment using Monte
14 Carlo simulations is also presented and discussed for
15 steady-state wear rate uncertainty analysis for an arbitrary
16 number of interrupted measurements of volume loss.

17
18 **Keywords** Wear · Wear rates · Uncertainty analysis

19 1 Introduction

20 Even in macroscopic tribology testing, there are numerous
21 experimental challenges in measuring and reporting both
22 friction coefficients [1, 2] and wear rates [3]. And while it
23 is common to make comparative statements about changes
24 in friction coefficient or wear rate of one experiment versus
25 another, the fact remains that in materials tribology some
26 portion of the sample is consumed during the experiment
27 and it is therefore impossible to have a standard artifact
28 that can be repeatedly interrogated. Thus, without the
29 ability to perform truly comparative analysis, it becomes

necessary to provide information regarding the uncertainty 30
in the measurement of friction coefficient and wear rate. 31

Wear data are collected to provide insights into wear 32
phenomena and to offer guidance to design engineers. 33
These data are typically presented as rates, and may 34
involve a single measurement of wear at the end of an 35
experiment or multiple measurements of wear during an 36
experiment. These results are influenced by the intrinsic 37
properties of the materials, the surface preparation, the test 38
conditions (mechanical, chemical, electrical, etc...) and the 39
measurement methods. In order to make defensible state- 40
ments regarding wear rate measurements, comparisons 41
between materials, or the dispersion of wear rate mea- 42
surements, it is essential to provide details about the 43
uncertainties in the measurements. 44

There have been past efforts to examine the sources of 45
variability in wear results. Almond and Gee [4] and Czi- 46
chos et al. [5] reported on inter-laboratory wear testing of 47
nominally identical material pairs and nominally identical 48
conditions, while Guicciardi et al. [6] conducted repeat 49
experiments with a single tribometer under controlled 50
conditions. Each study demonstrated significant variability; 51
not surprisingly, the results of intra-laboratory repeat 52
experiments varied less than inter-laboratory repeat tests. 53
Almond and Gee chose to ascribe the high inter-laboratory 54
variability in mass loss values to differences in the types of 55
test machines. In general, it is very difficult to determine 56
the relative contributions of materials properties, test con- 57
ditions, instrumentation, and measurement errors to 58
measurand variability without a detailed analysis of each 59
contributor. 60

Uncertainty analysis makes use of the *Law of Propa- 61*
gation of Uncertainty in order to characterize the disper- 62
sion of values that are reasonably attributed to the 63
measurand. In wear measurements, it is most common to 64

A1 D. L. Burris
A2 Department of Mechanical Engineering, University of Delaware,
A3 Newark, DE, USA

A4 W. G. Sawyer (✉)
A5 Department of Mechanical and Aerospace Engineering,
A6 University of Florida, Gainesville, FL 32611, USA
A7 e-mail: wgsawyer@ufl.edu

65 report a wear rate that follows Archard's wear equation
66 (Eq. 1):

$$\Psi = K F n d. \quad (1)$$

68 The traditional form (and units) for the wear rate, K ($\text{mm}^3/$
69 (Nm)), is the volume of material removed, Ψ (mm^3), per
70 unit normal load, FN (N), per distance of sliding, d (m). The
71 combined standard uncertainty, $u(K)$, requires knowledge
72 of the uncertainties for each of these terms. This article will
73 present three of the common methods used to compute wear
74 volumes and will then present methods to compute the
75 uncertainties in wear rate for single point and multiple point
76 measurements. This manuscript is in no-way exhaustive,
77 but aims to outline methods for determining the uncertainty
78 of the wear rate as a function of the uncertainties of the
79 measured input quantities. As discussed in earlier papers on
80 the topic by Schmitz et al. [3], information about the largest
81 contributors to the measurement uncertainty can be readily
82 used to aid in redesigning the experimental apparatus and/or
83 the procedure to reduce the measurement uncertainty.

84 2 Uncertainties in Wear Volume Measurements

85 In order to provide an uncertainty in a wear rate mea-
86 surement, the uncertainties in the force, sliding distance,
87 and wear volume must all be accounted for. There are a
88 number of different techniques that are used to measure or
89 infer the wear volume, and three of the most common
90 techniques are reviewed in this section. Depending on the
91 instrumentation design, it is possible that the uncertainties
92 in the normal load and sliding distance will also require an
93 additional analysis.

94 2.1 The Spherical Cap

95 Over the past 50 years, pin-on-disk experiments make
96 frequent use of a spherically capped pin as a standard
97 sample geometry. The pin effectively eliminates edge
98 contacts and provides a relatively straightforward mea-
99 surement of pin wear volume under situations that produce
100 flat circular wear scars on the end of the pin. Under such
101 situations, optical measurements of the resulting circular
102 flat spots are used to calculate the removed volume of
103 material. The exact solution for the volume of a spherical
104 cap with a height (h) on a sphere of radius (R) is given by
105 Eq. 2, and shown schematically in Fig. 1a:

$$\Psi = \frac{1}{3}\pi h^2(3R - h). \quad (2)$$

107 Since the height of the spherical cap cannot be measured
108 after wear tests, it is traditionally estimated using
109 trigonometric identities as shown in Eqs. 3 and 4:

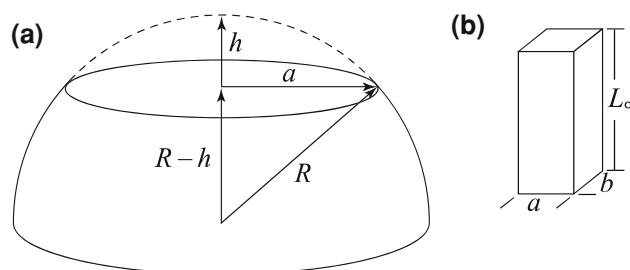


Fig. 1 Schematic and nomenclature for **a** the spherical cap wear measurement presented in Sect. 2.1, and **b** cuboidal sample presented in Sect. 2.2 and Sect. 2.3

$$R^2 = (R - h)^2 + a^2 = R^2 - 2Rh + h^2 + a^2, \quad (3)$$

$$2Rh = h^2 + a^2. \quad (4) \quad 111$$

It is common practice to keep the circular wear scars
113 much smaller than the radius of the pin ($a \ll R$). This has
114 lead to the order-of-magnitude assumptions made in Eqs. 5
115 and 6, which ultimately result in the approximate solution
116 given by Eq. 6. The first step is to recognize that $2R \gg h$,
117 which simplifies Eq. 4 to the approximate expression given
118 in Eq. 5:
119

$$h \cong \frac{a^2}{2R}. \quad (5)$$

Substitution of Eq. 5 into Eq. 2 gives an approximate
121 solution for the wear volume; this expression is further
122 simplified using order-of-magnitude approximations to
123 give the final form of the expression:
124

$$\Psi \cong \frac{1}{3}\pi \left(\frac{a^2}{2R}\right)^2 \left(3R - \frac{a^2}{2R}\right) \cong \frac{\pi a^4}{4R}. \quad (6)$$

This expression always under predicts the worn volume,
126 and the error from this approximation monotonically
127 increases with an increasing ratio of a/R reaching
128 approximately 10% at a value of $a/R = 0.5$; such large
129 values of a/R are easily avoided in practice. For the
130 uncertainty analysis, the approximate solution will be used,
131 and Eqs. 7 and 8 derive the uncertainty in wear volume for
132 the spherical cap:
133

$$\begin{aligned} u(\Psi)^2 &\cong \left(\frac{\partial \Psi}{\partial R}\right)^2 u(R)^2 + \left(\frac{\partial \Psi}{\partial a}\right)^2 u(a)^2 \\ &\cong \frac{\pi^2 a^8}{16R^4} u(R)^2 + \frac{\pi^2 a^6}{R^2} u(a)^2, \end{aligned} \quad (7)$$

$$u(\Psi)_{\text{spherical cap}} \cong \frac{\pi a^3}{4R^2} \sqrt{\left(a^2 u(R)^2 + 16R^2 u(a)^2\right)}. \quad (8) \quad 135$$

Commercially available spheres have excellent radial
137 tolerances (low uncertainty). It is very difficult to define an
138 uncertainty in the measurement of the wear scar diameter/
139 radius, and very often an average radius is estimated from
140

141 repeat measurements of different locations across the wear
142 scar (at the very least the uncertainty should be as large as
143 the standard deviation of these measurements). The
144 uncertainty in the measurement of the wear scar radius is
145 likely the dominant uncertainty contributor in the
146 calculated wear volume when using this approach.

147 2.2 Linear Displacement

148 Pin-on-disk experiments that use a sample with a uniform
149 cross-section can use a displacement measurement during
150 operation to calculate wear volumes assuming that all
151 deformations are due to wear (samples must be resistant to
152 creep). In low wear systems, this is tricky because of
153 temperature fluctuations that occur during the course of an
154 experiment. Additionally, the approach is only “accurate”
155 under conditions where wear is confined to one material
156 (often the pin). In this derivation, the volume loss and
157 associated uncertainties will be calculated assuming the pin
158 is the material that is wearing, and it has a square cross-
159 section with measured widths $a \cong b$ and an initial length
160 L_o ; this is shown schematically in Fig. 1b. The volume of
161 material removed (Ψ) is thus the difference between the
162 initial volume measurement and current volume measure-
163 ment, in which only the height of the sample is measured
164 again (i.e., the current volume is computed directly from a
165 measurement of the new specimen length L_f after assuming
166 that the lengths $a \cong b$ are unchanged). The expression for
167 volume loss is given by Eq. 9:

$$\Psi = ab(L_o - L_f). \quad (9)$$

169 Assuming that all of the dimensional measurements are
170 similar and were measured with the same instrument, it is
171 reasonable to assume that
172 $u(a) = u(b) = u(L_o) = u(L_f) = u(L)$; this simplifies the
173 expressions for the uncertainty derived in Eqs. 10–12:

$$u(\Psi)^2 \cong \left(\frac{\partial \Psi}{\partial a}\right)^2 u(L)^2 + \left(\frac{\partial \Psi}{\partial b}\right)^2 u(L)^2 + \left(\frac{\partial \Psi}{\partial L_o}\right)^2 u(L)^2 \\ + \left(\frac{\partial \Psi}{\partial L_f}\right)^2 u(L)^2, \quad (10)$$

$$175 \quad u(\Psi)^2 \cong \left(\left(\frac{\partial \Psi}{\partial a}\right)^2 + \left(\frac{\partial \Psi}{\partial b}\right)^2 + \left(\frac{\partial \Psi}{\partial L_o}\right)^2 + \left(\frac{\partial \Psi}{\partial L_f}\right)^2 \right) u(L)^2, \quad (11)$$

$$177 \quad u(\Psi)^2 \cong \left((b(L_o - L_f))^2 + (a(L_o - L_f))^2 + (ab)^2 + (ab)^2 \right) u(L)^2. \quad (12)$$

179 Under conditions where $a \cong b$ and $L_o \cong L_f$, Eq. 12 can be
180 further simplified to give the uncertainty in wear volume

$u(\Psi)$ in terms of the dimensions a and L_o , and the
181 difference $\Delta L = L_o - L_f$; this is given in Eq. 13: 182

$$u(\Psi)_{\Delta L} \cong \left(a\sqrt{2}\sqrt{\Delta L^2 + a^2} \right) u(L). \quad (13)$$

In low wear systems, it is quite common for the change
184 in length of the sample, ΔL , to be much smaller than the
185 width of the sample, a , and further simplification of Eq. 13
186 can be performed: 187

$$u(\Psi)_{\Delta L} \cong \sqrt{2} a^2 u(L). \quad (14)$$

2.3 Mass Loss

190 Mass loss measurements are widely used in polymer
191 tribology, where creep and plastic deformation of samples
192 under compressive and shear stresses make dimensional
193 measurements of the samples difficult. For materials that
194 do not change their mass due to outgassing or uptake of
195 fluids during testing this method can be particularly useful.
196 Calculations of volume loss and the relative uncertainties
197 associated with this method are discussed in detail in
198 Schmitz et al. [3] for a particular reciprocating tribometer
199 and laboratory instrumentation—the importance of a high
200 precision laboratory scale was clearly demonstrated. In the
201 mass loss method, the volume of material removed, Ψ , is
202 calculated from a measurement of the change in mass of the
203 sample, $\Delta m = m_i - m_f$, and the density of the sample ρ : 205

$$\Psi = \frac{m_o - m_f}{\rho} = \frac{\Delta m}{\rho}. \quad (15)$$

The density of the sample is computed through mass and
207 dimensional measurements made in the investigators’
208 laboratory. For this derivation, the pin sample is assumed
209 to have a square cross-section (as was assumed in
210 Sect. 2.2). Equation 15 is readily expanded to give an
211 expression for volume in terms of measured values as
212 shown in Eq. 16: 213

$$\Psi = \frac{\Delta m}{m_o/abL_o} = \frac{\Delta m ab L_o}{m_o}. \quad (16)$$

215 Again, we will assume that all of the dimensional
216 measurements are similar, and that $u(a) = u(b) = u(L_o)$
217 $= u(L_f) = u(L)$. We will also assume that the initial
218 and final masses are similar, and the associated uncertainties
219 are the same (i.e., $u(\Delta m) = \sqrt{2} u(m)$); this simplifies the
220 expressions derived in Eqs. 17–19:

$$u(\Psi)^2 = \left(\frac{\partial \Psi}{\partial \Delta m}\right)^2 u(\Delta m)^2 + \left(\frac{\partial \Psi}{\partial m_0}\right)^2 u(m_0)^2 + \left(\left(\frac{\partial \Psi}{\partial a}\right)^2 + \left(\frac{\partial \Psi}{\partial b}\right)^2 + \left(\frac{\partial \Psi}{\partial L_i}\right)^2\right) u(L)^2, \quad (17)$$

$$u(\Psi)^2 = \left(2 + \frac{\Delta m^2}{m_0^2}\right) \frac{(abL_0)^2}{m_0^2} u(m_0)^2 + ((a^2 + b^2)L_0^2 + a^2b^2) \frac{\Delta m^2}{m_0^2} u(L)^2. \quad (18)$$

The expressions are slightly more compact if $a \cong b$, as shown by Eq. 19, but considering the ease with which the uncertainties can be directly computed from the above expressions, it may not be of any tangible benefit:

$$u(\Psi)_{\text{mass loss}} = \frac{aL_0}{m_0} \sqrt{\left(\left(2 + \frac{\Delta m^2}{m_0^2}\right) a^2 u(m_0)^2 + \left(2 + \frac{a^2}{L_0^2}\right) \Delta m^2 u(L)^2\right)}. \quad (19)$$

2.4 Uncertainties in the Single Point Wear Rate Calculations

A single point measurement, for which the sample is measured once before and once after the test, is the most common method for quantifying wear rate, although it is inappropriate to refer to this as a steady-state wear rate. The expression for the single point wear rate K is given by Eq. 20:

$$K = \frac{\Psi}{Fn d}. \quad (20)$$

Dry sliding contacts have an initial transient period of wear during which the rates of wear are typically higher than those found in the steady-state. As a result, wear rate calculations from single point measurements are often artificially high. For this reason, and others, the method is not generally recommended.

The uncertainty $u(K)$ associated with single point wear rate calculations is derived in Eqs. 21–23. The uncertainties in volume loss, $u(\Psi)$, would be taken from the previous sections. The uncertainties in normal load, $u(Fn)$, and sliding distance, $u(d)$, may also require analysis:

$$u(K)^2 = \left(\frac{\partial K}{\partial \Psi}\right)^2 u(\Psi)^2 + \left(\frac{\partial K}{\partial Fn}\right)^2 u(Fn)^2 + \left(\frac{\partial K}{\partial d}\right)^2 u(d)^2, \quad (21)$$

$$u(K)^2 = \left(\frac{1}{Fn d}\right)^2 u(\Psi)^2 + \left(\frac{\Psi}{Fn^2 d}\right)^2 u(Fn)^2 + \left(\frac{\Psi}{Fn d^2}\right)^2 u(d)^2, \quad (22)$$

$$u(K) = \frac{1}{Fn^2 d^2} \sqrt{Fn^2 d^2 u(\Psi)^2 + \Psi^2 d^2 u(Fn)^2 + \Psi^2 Fn^2 u(d)^2}. \quad (23)$$

If the normal force is measured, then the uncertainty in the normal load is given by the manufacturer calibration of the force transducer. The sliding distance, d (m), is often computed by multiplying by the sliding speed V (m/s) and the duration of an experiment, t (s). For example, in rotating pin-on-disk experiments the circumference of the wear track $2\pi R_{\text{disk}}(m)$ and the number of revolutions per second (RPS) are used together to compute the sliding speed. The uncertainty in the sliding distance can be computed based on uncertainties in the test duration, wear track radius, and angular speed. Our experience has shown that the uncertainties associated with volume loss measurements dominate; to a good approximation, neglecting the uncertainty contributions from the normal load and the sliding distance has no discernable effect on the overall uncertainty.

3 Monte-Carlo Methods for Computing Wear Rate Uncertainties in Multiple Point Measurements

It is desirable to report steady-state wear rates, in part because they are used by engineers to make life prediction, but also because of the variability in the relatively short lived initial transients. This is typically done by performing a regression analysis through a set of data that has the volume loss plotted on the y -axis and the product of the normal load and sliding distance is plotted on the x -axis. The linear region of the data is selected and the slope of the least squares regression line is the steady-state wear rate. In order to report an uncertainty in the steady-state wear rate, it would thus be necessary to perform the uncertainty analysis on the least squares regression algorithm/expression. A numerical technique is a much simpler alternative, and can be performed in a variety of ways. An accepted technique is to perform a Monte-Carlo analysis on the data.

Performing a Monte-Carlo simulation to compute the uncertainties in the regression analysis of the steady-state wear rate requires the generation of a series of data sets (perhaps 10,000) that have the appropriate mean and standard deviation in volume loss and the product of normal load and sliding distance. Essentially, each data point collected during the experiment is numerically perturbed according to an appropriate random process. One way to do this is to generate a field of random numbers (remember to use a Gaussian random number generator) with a mean value of zero and a standard deviation that is equal to the uncertainty in that point; the measured value is then added

299 to each of these numbers, which results in a field of
 300 numbers with the appropriate statistics. Once this field of
 301 numbers has been generated, a series of regression analyses
 302 are completed. The mean slope from this regression analysis
 303 is the steady-state wear rate, and the standard deviation
 304 of these slopes is the uncertainty in the steady-state wear
 305 rate.

306 **4 Example Calculations**

307 Example calculations of uncertainty in wear rate are shown
 308 graphically in Fig. 2. Data from Burris and Sawyer [7] are
 309 used. Briefly, the experimental setup was a reciprocating
 310 pin-on-disk tribometer that had an average normal load of
 311 250 N and a sliding speed of 50 mm/s. The samples were
 312 machined from a bulk nanocomposite of PTFE and alumina
 313 into cuboidal samples (shown in Fig. 2a). The dimensions
 314 of the sample and the associated uncertainties are given in
 315 Fig. 2a. The 50 μg (5 × the scale resolution)
 316 mass measurement uncertainty reported by Burris and

Sawyer [7] is used in this analysis. The uncertainties in the
 317 sliding distance and normal load are exaggerated here by
 318 nearly an order-of-magnitude to make them visible in the
 319 graphical representation of the data shown in Fig. 2b.
 320

Examining Fig. 2b, it is clear that this sample experi-
 321 enced a substantial transient wear process. The data are
 322 comprised five sequential mass measurements. If the last
 323 measurement were used to compute a single point wear
 324 rate, the wear rate would be $K = 2.42 \times 10^{-6} \text{ mm}^3/(\text{Nm})$
 325 as given by Eq. 24:
 326

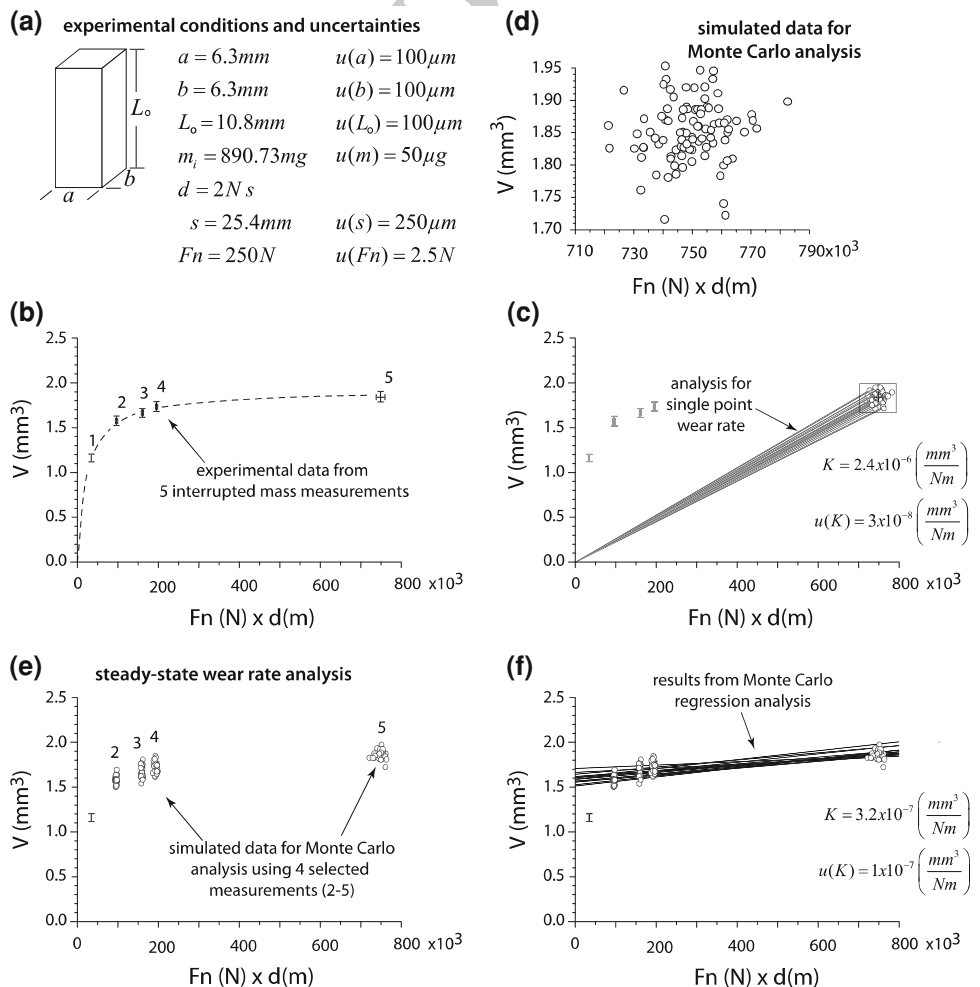
$$K = \frac{V}{Fn d} = \frac{\Delta m a b L_o}{m_o F n d}$$

$$= \frac{3.83 \text{ mg}}{890.79 \text{ mg}} \frac{6.3 \text{ mm} \cdot 6.3 \text{ mm} \cdot 10.8 \text{ mm}}{250 \text{ N} \cdot 3,048 \text{ m}}$$

$$= 2.42 \times 10^{-6} \frac{\text{mm}^3}{\text{Nm}} \quad (24)$$

Following the analysis presented in Sect. 2.3, the
 328 uncertainty in the volume of material removed, $u(V)$, is
 329 0.056 mm^3 ; this is approximately 3% of the calculated
 330 mass loss ($V = 1.84 \text{ mm}^3$). This calculation is given by
 331 Eqs. 25 and 26:
 332

Fig. 2 Experimental data taken from Burris and Sawyer [7]: **a** experimental sample geometry, nomenclature, nominal measurements, and associated uncertainties, **b** plot of five interrupted measurements, **c** graphical representation of the single point uncertainty calculation, **d** simulated data of the final measurement, **e** steady-state analysis requires a set of simulated data for each experimental data point included in the Monte-Carlo simulation, and **f** graphical representation of the Monte-Carlo simulation for wear rate uncertainty analysis



$$u(V) = \frac{6.3 \text{ mm } 10.8 \text{ mm}}{890.73 \text{ mg}} \sqrt{\left(\left(2 + \frac{3.83^2}{890.73^2} \right) 6.3^2 0.050^2 + \left(2 + \frac{6.3^2}{10.8^2} \right) 3.83^2 0.1^2 \right) \text{mg}^2 \text{mm}^2}, \quad (25)$$

$$u(V) = \frac{68.04 \text{ mm}^2}{890.73 \text{ mg}} \sqrt{((2)0.1 + (2.34)0.146) \text{mm}^2 \text{mg}^2} \\ = 0.056 \text{ mm}^3. \quad (26)$$

334 Following the analysis for the uncertainty in single point
335 wear rates presented and discussed in Sect. 3.0, the
336 uncertainty in the wear rate is $u(K) = 3 \times 10^{-8} \text{mm}^3/$
337 (Nm). In this example, the uncertainty in normal load is
338 $u(Fn) = 2.5 \text{N}$ and the uncertainty in the sliding distance is
339 $u(d) = 2N u(s) = 30 \text{m}$, where the number of reciprocating
340 cycles, N , is known exactly but there is uncertainty in the
341 reciprocating stroke length $u(s) = 250 \mu\text{m}$. These
342 calculations are shown in Eqs. 27 and 28, where Eq. 27
343 is taken from Eq. 23:

$$u(K) = 3 \times 10^{-8} \frac{\text{mm}^3}{\text{N m}}. \quad (28)$$

$$u(K) = \frac{\sqrt{(250^2 3,048^2 0.056^2 + 1.84^2 3,048^2 2.5^2 + 1.84^2 250^2 30^2) \text{N}^2 \text{m}^2 \text{mm}^6}}{250^2 \text{N}^2 3,048^2 \text{m}^2}, \quad (27)$$

345 This analysis is shown graphically in Fig. 2c, where a
346 scatter plot of simulated data with the appropriate statistics
347 is shown in place of the measured value and experimental
348 uncertainties (Fig. 2d). This, in effect, is the technique that
349 would be used for a Monte-Carlo simulation of a single
350 point wear rate assuming no uncertainty in the starting
351 value. The average wear rate would then be the average of
352 the slopes of the lines from the origin to the simulated data
353 point and the uncertainty would be the standard deviation
354 in these slopes; these converge upon the analytical values
355 from Eqs. 20 and 23 as the number of simulated points
356 approaches infinity.

357 Computing the wear rate and the associated uncer-
358 tainties in the steady-state wear rate proceeds in the same
359 fashion as previously discussed. Namely, the data points
360 that represent the steady-state region are selected; for this
361 example, points 2, 3, 4, and 5 are chosen. Simulated data
362 with the appropriate statistics are created in an uncorrel-
363 ated fashion (a random number with the appropriate

Gaussian distribution is used) and plotted as shown in 364
Fig. 2e (for this example, a thousand points were gen- 365
erated but it is not unusual to generate 10,000 or more 366
points). Regression analyses are performed on the 1,000 367
data sets that are selected randomly from the simulated 368
data points. The average wear rate is found to be 369
 $K = 3.2 \times 10^{-7} \text{mm}^3/(\text{Nm})$ with an uncertainty of 370
 $u(K) = 1 \times 10^{-7} \text{mm}^3/(\text{Nm})$. As previously discussed, 371
the steady-state wear rate is less than the single point 372
wear rate, and interestingly has a larger uncertainty pri- 373
marily due to the dispersions of data in the points 2, 3, 374
and 4, which so strongly influence the regression analy- 375
sis. An approach that would improve this experimental 376
design would be to collect more points between points 4 377
and 5, or space the collected data more evenly through- 378
out the experiment. 379

5 Concluding Remarks 380

A defensible statement of measurement uncertainty is crit- 381
ical to the analysis of data dispersion; this is especially 382
important for wear rates, for which orders-of-magnitude 383
variations are common. Frequently, the uncertainties in low 384
wear rate materials are on the same order of magnitude as 385
the measurement; these uncertainties should be reduced 386
before comparisons and discussions of differences are dis- 387
cussed. The relative ease with which Monte-Carlo simula- 388
tions can be performed permits direct computations of 389
uncertainties for either single-point or steady-state wear 390
rates without mathematical derivations; this is especially 391
important for a wide array of systems, which exhibit tran- 392
sient wear behavior. 393

Acknowledgments Financial support for this work was provided 394
through an AFOSR-MURI grant FA9550-04-1-0367. We would also 395
like to thank Prof. T. L. Schmitz and Prof. J. C. Ziegert for many 396
helpful discussions regarding tribometry and uncertainty analysis. 397

398 **References**

- 399 1. Schmitz, T.L., Action, J.E., Ziegert, J.C., Sawyer, W.G.: The
400 difficulty of measuring low friction: uncertainty analysis for
401 friction coefficient measurements. *J. Tribol.* **127**, 673–678 (2005)
402 2. Burris, D.L., Sawyer, W.G.: Addressing practical challenges of
403 low friction coefficient measurements. *Tribol. Lett.* **35**, 17–23
404 (2009)
405 3. Schmitz, T.L., Action, J.E., Burris, D.L., Ziegert, J.C., Sawyer,
406 W.G.: Wear-rate uncertainty analysis. *J. Tribol.* **126**, 802–808
407 (2004)
4. Almond, E.A., Gee, M.G.: Results from a UK interlaboratory
project on dry sliding wear. *Wear* **120**, 101–116 (1987) 408
5. Czichos, H., Becker, S., Lexow, J.: Multilaboratory tribotesting:
results from the Versailles-advanced-materials-and-standards-pro-
gram on wear test methods. *Wear* **114**, 109–130 (1987) 409
6. Guicciardi, S., Melandri, C., Lucchini, F., de Portu, G.: On data
dispersion in pin-on-disk wear tests. *Wear* **252**, 1001–1006 (2002) 410
7. Burris, D.L., Sawyer, W.G.: Tribological sensitivity of PTFE/
alumina nanocomposites to a range of traditional surface finishes.
Tribol. Trans. **48**, 147–153 (2005) 411
412
413
414
415
416
417
418

UNCORRECTED PROOF